Polymer 123 (2017) 55–64

Contents lists available at ScienceDirect

Polymer

journal homepage: www.elsevier.com/locate/polymer

Continuous fabrication of cellulose nanocrystal/poly(ethylene glycol) diacrylate hydrogel fiber from nanocomposite dispersion: Rheology, preparation and characterization

Kai Hou [a], Yan Li [a], Yao Liu [a], Ruihui Zhang [a], Benjamin S. Hsiao [b], Meifang Zhu [a, *]

[a] State Key Laboratory for Modification of Chemical Fibers and Polymer Materials, College of Materials Science and Engineering, Donghua University, 2999 North Renmin Road, Shanghai, 201620, People's Republic of China
[b] Department of Chemistry, Stony Brook University, Stony Brook, NY 11794, USA

ARTICLE INFO

Article history:
Received 18 April 2017
Received in revised form
15 June 2017
Accepted 17 June 2017
Available online 29 June 2017

Keywords:
Dynamic crosslinking spinning
Nanocomposite hydrogel fiber
Cellulose nanocrystals

ABSTRACT

Advances in hydrogel design are yielding new hydrogel materials with diverse macroscopic topological structures. Among these, hydrogel fibers have been considered as a new class of hydrogel material with unique spatiotemporal properties. In this study, based on the novel non-template dynamic-crosslinking-spinning (DCS) method which has been demonstrated for scalable fabrication of size-controllable hydrogel fibers from oligomers, the method involved the use of one-step production of nanocomposite hydrogel fiber with weakly-gelled nanoparticle/oligomer (cellulose nanocrystals/poly(ethylene glycol) diacrylate, CNC/PEGDA) dispersion, where the interparticle interactions between CNC dominate the rheological property. The weakly-gelled CNC/PEGDA dispersion exhibited viscoelastic and shear thinning behavior, where continuous and uniform CNC/PEGDA hydrogel fibers were successfully fabricated by controllable extrusion. The diameter and water retention of the fibers could be controlled by the CNC content and spinning parameters. In addition, mechanical properties of the fiber were found to increase in the presence of CNC.

1. Introduction

Hydrogel, a class of unique soft material, has been exploited in many research activities and industrial applications, due to their tunable and distinctive properties, such as highly water retention, porous structure, ease functionalization, stimuli-responsive property and etc [1–5]. Advances in hydrogel design have led to the development of a new generation of hydrogel materials with diverse macroscopic structures, such as gradient porous [6], knitted [7], patterning [8], ordered porous structure [9], and sandwich structures [10]. These structures often exhibit anisotropic properties in swelling or stimuli-responsiveness. Among these, hydrogel fiber is a unique one-dimensional material with spatiotemporal properties such as high length/diameter ratio, flexibility and knittability (reconstructed into 2D and 3D structure), which are suitable for applications in biomimetic device [11], biomaterial [12], signal transmission media [13] and etc.

Polymers that are suitable for hydrogel fiber production should possess water-soluble linear chains and high molecular weight, such as alginate or ultra-high molecular weight polyoxyethylene [14–16]. However, scalable hydrogel fiber production, starting from monomers or oligomers (the common functional and structural element of hydrogel), presents many challenges. One of the important challenges is in the aspect of time consideration. As spinning is a dynamic process, in which the solid fiber segment forms instantaneously with anisotropic molecular order under uniaxial drawing force [17]. Conversely, fabrication of hydrogel fiber by the in-situ polymerization process must also consider the additional factor of polymerization kinetics. In specific, one demonstrated hydrogel fiber fabrication method using in-situ polymerization with slow kinetics in capillary could only produce limited fiber length and not be able to be produced continuously in a large scale [13,18].

Recent advances in polymer chemistry and micro-device using pre-gel monomer solutions appeared to be able to overcome the continuous spinning challenge. This is because the rapid polymerization process could lead to instantaneous fiber formation [19]. Furthermore, microfluidic technology combining with rapid

* Corresponding author.
E-mail address: zhumf@dhu.edu.cn (M. Zhu).

http://dx.doi.org/10.1016/j.polymer.2017.06.034
0032-3861/

photopolymerization have been exploited for continuous production of hydrogel fiber [20]. Comparing with the use of capillary, the microfluidic device is a much desirable and sophisticated chemical reactor, in which dynamic polymerization can be precisely controlled with the design geometry and the use of pre-gel solution. However, the application of microfluidic device as reactor for mass production of hydrogel fiber is still not practical due to the complexity of the design and operation of microfluidic devices.

The non-template method has been showed to be a convenient way to fabricate hydrogel fiber, but it relies on the proper viscoelastic property of pre-gel solution. Several non-template methods have exploited pre-crosslinked (covalent or non-covalent) dispersions in hydrogel fiber production. For example, a Chinese-noodle-inspired extrusion process [21] has been demonstrated for hydrogel fiber fabrication using a covalently crosslinked dispersion. In this study, the aqueous pre-gel solution was filled in a syringe and exposed to the UV light for polymerization. And then the pre-crosslinked hydrogel was extruded through a sieve with specific diameter to obtain noodle-like hydrogel. However, this two-step process (polymerization and extrusion) was found difficult to produce fiber continuously.

Using nanocomposite pre-gel suspension, a hydrogel fiber textile was successfully demonstrated by 3D printing [11] using the following fabrication process. A clay/monomer nanocomposite dispersion was extruded directly on a platform with specific designed pattern and then photopolymerized to form hydrogel fiber textile. In this method, clay strongly interacted with monomer in a non-covalent manner as a rheological thickener, which led to the gelation of clay/monomer dispersion (storage modulus (G′) higher than loss modulus (G″)) and ensured that the extruded dispersion was not deformed before polymerization. The addition of rheological thickener inspired us to explore a new way to control the viscoelastic property of dispersion to tailor the fabrication of nanocomposite hydrogel fiber, since the nanocomposite hydrogel have exhibited superior properties to traditional organogel without nanofillers [22–25].

In our previous research, on the basis of wet-spinning, we have demonstrated a novel non-template dynamic-crosslinking-spinning (DCS) method and successfully spun organogel fiber in a large scale with controllable diameter using poly(ethylene glycol) diacrylate (PEGDA) oligomer [26]. This research confirmed the spinnability of aqueous oligomer solution through rapid polymerization under drawing force. In the current study, we aimed to demonstrate a new paradigm of using the DCS approach to fabricate nanocomposite hydrogel fiber. In specific, we used cellulose nanocrystals (CNC) as the nanofiller and successfully produced CNC/PEGDA hydrogel fiber. The rheological measurement of pre-gel dispersion revealed that the neat PEGDA oligomer solution (Newtonian fluid) transformed into polymer-like solution (non-Newtonian or pseudo-plastic fluid) after the addition of CNC. The pre-gel dispersion showed weak gelation behavior and distinct shear thinning property, which could be adjusted by extrusion conditions for spinning. Moreover, we demonstrated the diameter and water retention property of the fiber could be controlled by spinning parameters, and the mechanical property was significantly improved by addition of CNC in a proper concentration. In summary, DCS method is an effective approach to produce nanocomposite hydrogel fibers, which provide a method to utilize hydrogel fibers as carrier of functional nanoparticles with photocatalysis [27–29], photo-thermal [30,31] and other properties [32,33].

2. Experimental

2.1. Materials

Cellulose nanocrystals (CNC) was supplied by Guilin Qihong Technology Co. Ltd. and the sample was purified by dispersion-centrifugation (Centrifuge 5804R, Eppendorf, Germany; 10000r/min for 1 h to obtain CNC sediment) for 3 times. Finally, the purified CNC powder was obtained by lyophilization (LyoQuest-85, Telstar, Spain). Poly(ethyleneglycol) diacrylate (PEGDA, Mn = 700) and photoinitiator 2-Hydroxy-4'-(2-hydroxyethoxy)-2-methylpropiophenone (IRGACURE 2959, I2959, 98%) were obtained from Sigma-Aldrich. Karl-Fisher solution (pyridine-free) was purchased from Sino-pharm Chemical Reagent Co. Ltd. Deionized water was made by a water purification system (Heal Force Bio-Meditech Holdings Ltd).

2.2. Fabrication of CNC/PEGDA hydrogel fibers

CNC dispersion was obtained by dissolving CNC powder in deionized water and under stirring for 24 h. And then the mixture of I2959 and PEGDA (I2959: PEGDA = 5: 1000, wt%) was added into the CNC dispersion under continuous magnetic stirring at room temperature (25 °C) avoiding light for 24 h to get uniform pre-gel dispersion, which was subsequently utilized for dynamic-crosslinking-spinning (DCS). Pre-gel dispersions with different components are shown in Table 1.

The spinning procedure of CNC/PEGDA hydrogel fiber was similar to our previous work [26]. In brief, the pre-gel dispersion was extruded into the water bath (25 °C) perpendicularly through a cylindrical nozzle by metering pump (KDS100, KD Scientific, USA). Diameter of nozzle could be changed in order to adjusting the shear rate. Mercury lamp UV irradiation (S1500, EXFO, Canada. $\lambda = 360$ nm, 2.77w/cm^2) was used to initiate photopolymerization of the extruded dispersion in water, resulting in continuous formation of cylindrical hydrogel dynamically. The cylindrical hydrogel was continuously collected on a plastic roller outside the bath to form hydrogel fiber, where the collecting roll possessed a range of adjustable winding speed (0–1000 m/h) that could be used to apply varying drawing force to reduce the fiber diameter.

2.3. Characterization of pre-gel dispersion and hydrogel fibers

The rheology property of pre-gel dispersions was tested by a rotational rheometer (ARES, TA, USA) at 25 °C. The parallel plate mode (50 mm) with a sample gap of 600 μm was adopted. The dynamic frequency sweep measurement was performed at the strain of 1%. The shear rate range for steady mode was from 10^{-1} s^{-1} to 10^3 s^{-1}. The structure of hydrogel fiber was characterized by attenuated total reflectance Fourier transform infrared spectroscopy (ATR-FTIR, Nicolet 6700, Thermo Fisher, USA. Wavenumber range from 4000 to 600 cm^{-1}) and X-ray diffraction (XRD, D/max-2550 PC, Rigaku, Japan). The as-prepared fibers were soaked in pure

Table 1
CNC/PEGDA dispersion with different component.

Solution/Sample No.	CNC (wt%)	PEGDA and I2959 (wt%)	Water (wt%)
C_0P_{70}	0	70	30
$C_{0.3}P_{70}$	0.32	70	29.68
$C_{0.6}P_{70}$	0.64	70	29.36
$C_{0.9}P_{70}$	0.95	70	29.05
$C_{1.2}P_{70}$	1.27	70	28.73
C_4P_0	4	0	96

water for 24 h to remove impurities and then lyophilizated for ATR-FTIR and XRD measurements. The image of CNC nanoparticle was taken by transmission electron microscope (TEM, JEOL 2100) and field emission scanning electron microscopy (FE-SEM, S4800, Hitachi, Japan). Surface structure of fibers was characterized by scanning electron microscopy (SEM, JSM-5600LV, Nippon-optical, Japan). The morphology of cross-section of fiber was observed by field emission SEM (FE-SEM, S4800, Hitachi, Japan). Diameters and mechanical property of as-prepared fibers were measured by optical microscopy (VHM2600, VIHENT, China) and monofilament tensile testing machine (YG004, Changzhou Dahua Electronic Instrument Co. Ltd, China), respectively. The mean values of 10 fibers were reported. Water retention of the fiber was detected by the Karl-Fischer coulomb titration system (MA-1, BENON, China).

3. Results and discussion

3.1. Rheology of pre-gel dispersions

Previously, we have confirmed that the proper viscoelasticity of PEGDA is crucial for the DCS operation to maintain the filament-shape oligomer phase after extrusion into the water bath [26]. In this study, comparing with the neat PEGDA aqueous solution, large amount of hydrogen bond was formed (Fig. 1) between the hydroxyl groups on CNC and the carbonyl groups on PEGDA. In order to quantitatively analysis the influence of hydrogen bond on viscosity of the CNC/PEGDA dispersion, rheological characterization was carried out and the results are shown in Fig. 2.

Transformation of storage modulus (G′) and loss modulus (G″) during the frequency-dependent oscillatory rheological measurement were utilized to examine the stability change of material in sol-gel transition process. Typically, G′ above G″ means that the elasticity is dominant, which implies the gelation process is prevailing. In contrast, G″ above G′ represents a viscosity dominated solution-like material. In Fig. 2a, for the C_0P_{70} sample, the G′ was lower than G″ in the whole frequency range (0.1–100 rad s^{-1}), which indicates a typical solution behavior. By contrast, neat CNC dispersion (C_4P_0) showed a typical gel-like property (G′ above G″), where both G′ and G″ remained about constant in the whole frequency range (0.1–100 rad s^{-1}). This may be because that the network of neat CNC dispersion was formed by particle interactions, which confined the spatial movement of CNC under oscillation. However, the mixture showed a different behavior. The homogeneous CNC/PEGDA pre-gel dispersion ($C_{1.2}P_{70}$) exhibited simultaneous increasing of both G′ and G″ values, quite different than those of neat PEGDA. Interestingly, G′ increased faster than G″, indicating the gelation tendency of CNC/PEGDA dispersion because of the non-covalent interaction between CNC and PEGDA. Comparing with neat PEGDA, the CNC/PEGDA dispersion displayed reduced frequency dependence of G′ and G″ in the low frequency range, implying the transition from solution-like to gel-like viscoelastic property [39].

The loss factor ($\tan\delta = G''/G'$) represents the ratio of lost energy to storage energy during deformation. Comparing with the neat PEGDA oligomer solution, quantity of tanδ (Fig. 2b) of $C_{1.2}P_{70}$ is much lower, which confirms that the addition of CNC resulted in the increasing of elastic property more obviously than viscous property. Further, tan δ of $C_{1.2}P_{70}$ became nearly stable and almost independent of frequency as the neat CNC dispersion (its tanδ is nearly independent with frequency, especially at a low frequency range). These results confirmed the occurrence of sol-gel transition in CNC/PEGDA dispersion. Furthermore, the observation of a tanδ value of about 0.1 and its low frequency dependence indicates that the system is a weak gel, which has been observed in different systems [34,35].

The addition of CNC can clearly control the gelation process of PEGDA oligomer solution. The obvious effect of the gelation tendency in CNC/PEGDA dispersion is the viscosity increase that would be disadvantageous for spinning [36]. This is because high viscosity would restrict the motion and orientation of molecular chain under drawing during spinning. Moreover, high viscosity would also lead to extrusion swelling at the nozzle, which is one of the main challenges in fiber fracturing during spinning. To fine tune the spinnability of the CNC/PEGDA pre-gel dispersion, which was also characterized by the steady shear measurement. In Fig. 2c, it was found that the linear correlation between the shear rate ($\dot{\gamma}$) and shear stress (τ) of the neat PEGDA solution (C_0P_{70}) indicated a Newtonian fluid behavior because the PEGDA oligomer is a low molecule weight compound. In contrast, the CNC/PEGDA pre-gel dispersion exhibited the non-Newtonian behavior having a power

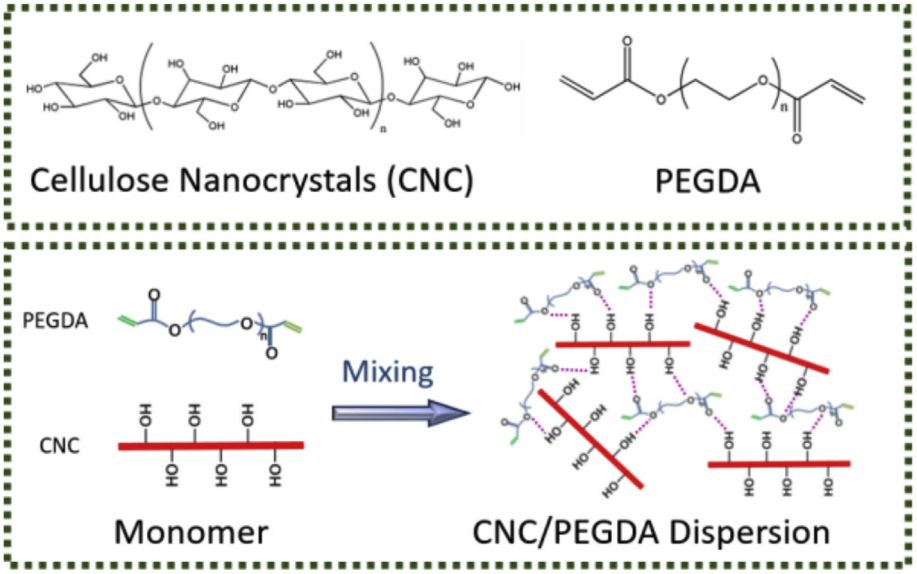

Fig. 1. Chemical structure and schematic illustration of the interaction between cellulose nanocrystals (CNC) and PEGDA in aqueous dispersion.

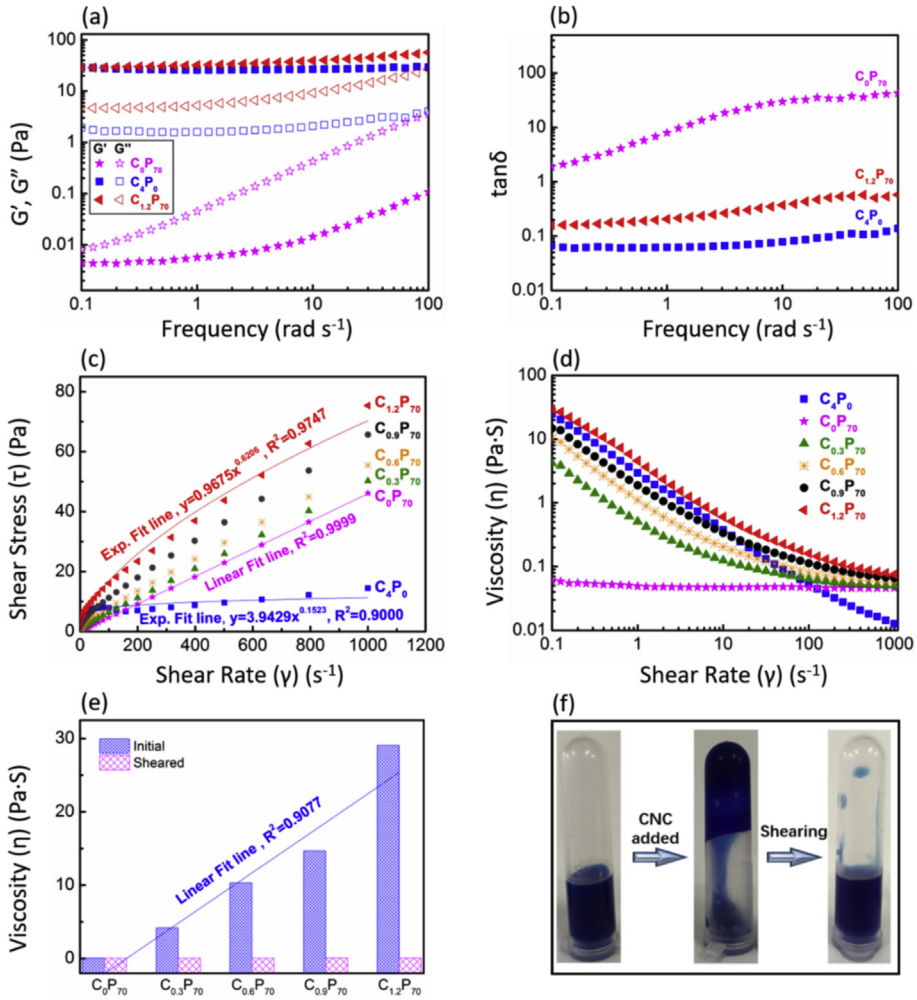

Fig. 2. Rheological property of the CNC/PEGDA dispersion. (a) Frequency dependence of the storage modulus (G′) and loss modulus (G″) of neat CNC, PEGDA and CNC/PEGDA dispersions. (b) Frequency dependence of the loss factor (tanδ) of neat CNC, PEGDA and CNC/PEGDA dispersion. (c) Shear rate dependence of shear stress and (d) viscosity as a function of CNC content for CNC/PEGDA dispersion. (e) CNC content dependence of initial and sheared viscosity. (f) Viscosity change of the dispersion after shear (dyed by methylene blue). (For interpretation of the references to colour in this figure legend, the reader is referred to the web version of this article.)

law relationship [37]:

$$\tau = K\dot{\gamma}^n$$

This equation is the classical relationship between shear rate and shear stress for pseudo-plastic fluid, where K is the consistency index and n is the non-Newtonian index.

Typically, polymer solution with chains larger than the entanglement molecular weight would behave as a pseudo-plastic fluid because of the chain entanglement. However, in CNC/PEGDA dispersion, although the PEGDA chain length is below the entanglement molecular weight, the long aspect ratio of CNC (the mean fiber diameter of CNC was 9.0 ± 2.6 nm and the mean fiber length was 215.6 ± 24.9 nm, Fig S1 shows.) and interaction of CNC/PEGDA can provide a different means to gel the suspension. The addition of CNC can form a network structure in the CNC/PEGDA dispersion with rheological property similar to polymer solution. It was interesting to find that the non-Newtonian index n was a negative value, and was a function of the CNC content. The increasing CNC content (i.e., 0.3, 0.6, 0.9, 1.2 wt%) led to decreasing n value (0.9054, 0.8361, 0.7477, 0.6206, respectively). The trend of the n change indicates the transition from the Newtonian to pseudo-plastic liquid behavior of the CNC/PEGDA dispersion, where the increase in the CNC content led to dominant pseudo-plastic liquid behavior [38].

The viscosity of the CNC/PEGDA dispersion with different CNC content is shown in Fig. 2d. It was found that the viscosity of neat PEGDA was independent of the shear rate, whereas all CNC/PEGDA dispersions exhibited notable shear thinning behavior. In polymer solutions, the shear thinning behavior can be attributed to the disentanglement and orientation of polymer chains under flow. However, shear thinning in CNC/PEGDA is mainly caused by the collapse of weak-gel network formed by CNC particles and PEGDA oligomer. This behavior has been reported in the systems of nanocomposite suspension [11,39]. In was interesting to note that the CNC content was linearly correlated with the initial viscosity (or approximate zero-shear viscosity) with a positive slope (Fig. 2e). This finding is consistent with the notion that the rheological property of the CNC/PEGDA dispersion was mainly dependent on the particle interactions of CNC. However, when the shear rate was increased to 1000 s^{-1}, the viscosities of the dispersions with different CNC contents became nearly identical, and this value was similar with the viscosity of neat PEGDA. This suggests that the network structure of CNC particles was completely destroyed, and the viscosity was mainly dominated by the oligomer content.

To maintain good spinning stability, an appropriate viscosity

range of the nanocomposite dispersion is essential for the extrusion and stretching operations. For example, suspension with low viscosity could not sustain the drawing force and lead to fracture, while suspension with very high viscosity could not be extruded easily. Therefore, adjusting the suspension viscosity to a proper range is an important step to reach continuous spinning. Typically, the viscosity (η) of the Newtonian fluid passing through a capillary can be adjusted by shear rate ($\dot{\gamma}$), which can be expressed by the following equation:

$$\dot{\gamma} = \frac{4Q}{\pi r^3}$$

where Q is the volume flow rate and r is the inner radius of the capillary. For a non-Newtonian fluid, this equation can be modified as follow:

$$\dot{\gamma}^* = \frac{3n+1}{4n}\dot{\gamma}$$

$\dot{\gamma}^*$ is the shear rate of the pseudo-plastic liquid flowing through a capillary, n is the non-Newtonian index. Therefore, this result provides us an effective way to control the viscosity of the CNC/PEGDA dispersion suitable for spinning by adjusting the nozzle diameter and extrusion rate. The viscosity of CNC/PEGDA dispersion under different spinning condition was calculated, and the results are shown in Table S1. The viscosity change of the dispersion after the CNC addition can be illustrated in Fig. 2f. It was seen that in the presence of CNC, a transition from solution state to a gel-like state occurred, where the flowability of the CNC/PEGDA dispersion dramatically reduced. However, the CNC particulate network could be easily broken under shear, where the viscosity of the CNC/PEGDA dispersion was deceased by shear.

3.2. Fabrication and morphology of hydrogel fibers

Dynamic-crosslinking-spinning (DCS) technology we established before has been shown as an effective method to produce hydrogel fiber using Newtonian fluid (PEGDA). Now we further demonstrated that CNC/PEGDA nanocomposite hydrogel fiber could also be fabricated by the DCS method using nanocomposite dispersion with gelation tendency.

As Fig. 3 illustrates, in brief, the shear force in the extrusion process could reduce the viscosity of the CNC/PEGDA dispersion in the gel state. As a result, a filament-shape CNC/PEGDA fluid phase was formed after extruded into water due to the proper viscoelasticity of CNC/PEGDA dispersion. Instantaneous photopolymerization was triggered by UV irradiation on the fluid phase, which was rapidly solidified into a hydrogel filament. With the dynamic extrusion approach, the filament-shape CNC/PEGDA hydrogel could be collected continuously out of water by a roller. In this approach, it is important that the UV light irradiated on the downstream of extruded dispersion, not at the nozzle, to maintain the fluidity of filament-shape phase. The main reason for this step is that, comparing with the solidified hydrogel fiber, the fluid phase has better deformability to release the tension generated by the drawing force to ensure the continuity of spinning.

The morphologies of the surface and cross-section of the hydrogel fiber are shown in Fig. 4 using scanning electron microscopy (SEM). In Figs. 4a1, it was seen that the fiber alignment was regular and the fiber diameter was also uniform, confirming the stability of DCS method for producing large scale nanocomposite CNC/PEGDA hydrogel fiber. Fig. 4a2 & 4a3 illustrate the surface morphology of CNC/PEGDA hydrogel fiber with different magnifications. The rough wrinkle on the surface could be attributed to the collapse of the internal pores, caused by lyophilization that was common in the PEG-based hydrogel [20].

The morphology of cross-section of fibers is illustrated in Fig. 4b with different magnifications. Different from the fiber produced by traditional wet spinning, of which the fiber-forming is driven by double diffusion of solvents (i.e., different solvents in the spinning solution and coagulating bath, where they mutually diffuse into each other to induce the polymer coagulation), which always generates irregular cross-section shape [17]. As for our DCS method, no double diffusion occurred because the solvent of dispersion and coagulating bath was water. Moreover, photopolymerization was so rapid that the cylindrical shape of extruded dispersion could be maintained after solidification. As the network of solidified hydrogel fiber had poor deformability under drawing force, the hydrogel fiber spun by DCS possessed regular round cross-section resembled the shape of cylindrical nozzle. The higher resolution cross-section image in Figs. 4b3 indicated that the distribution of CNC in the hydrogel fiber was homogeneous, suggesting that both shear stress and drawing force did not affect the distribution of CNC, which was beneficial for the mechanical property enhancement of hydrogel fibers. The above results confirmed that non-covalent cross-linked CNC/PEGDA dispersion could be utilized in to produce continuous and uniform hydrogel fiber by the versatile DCS method suitable for one-component or multi-component solution.

Fig. 5a displays the XRD patterns profiles of CNC powder and CNC/PEGDA hydrogel fiber, respectively. As for the CNC powder, a series of diffraction peaks at 14.9°, 16.3°, 22.7° and 34.4°, characteristic of the 101, 101′, 002 and 040 crystalline planes of CNC, were observed [40]. The XRD pattern for CNC/PEGDA hydrogel fiber was found to be dramatically affected by the presence of PEGDA, where only a single broad peak, ranging from 10° to 35°, characteristic of the disordered microstructure of the amorphous domain, was seen. This observation could be explained by the small content of CNC in the fiber and the large exfoliation of nanoparticles [39,41].

The FTIR spectroscopy results are shown in Fig. 5b. As for neat CNC, the characteristic peaks at 3332 cm^{-1} and 667 cm^{-1} represented the hydrogen bonded stretching of -OH and C-OH out of plane bending, respectively, whereas peak at 2899 cm^{-1} could be assigned as the C-H stretching, peak at 1429 cm^{-1} was H-C-H and O-C-H in-plane bending vibration [40]. As for PEGDA oligomer, the characteristic peaks at 1636 cm^{-1} and 986 cm^{-1} represented the stretching vibration of C=C of acrylate, absorption band at 1110 cm^{-1} and 1725 cm^{-1} was attributed to the stretching vibration of C-O-C and C=O, respectively [42]. As for CNC/PEGDA hydrogel fiber, the disappearance of peaks at 1636 cm^{-1} and 986 cm^{-1} indicated that polymerization occurred between the C=C double bond of PEGDA. The characteristic peaks of CNC at 3344 cm^{-1} and 669 cm^{-1} suggested that CNC composed into the hydrogel matrix homogeneously.

3.3. Diameter control of hydrogel fibers

In our earlier study, we showed that the primary advantage of DCS method is the precision control of hydrogel fiber diameter [26]. In specific, the cross-sectional area could be linearly correlated with the oligomer concentration, extrusion rate and winding speed by this approach, where these relationships have been summarized for hydrogel fiber spun from a Newtonian fluid (i.e., neat PEGDA solution). In the current study, in order to investigate the influence of CNC addition on the fiber diameter, groups of hydrogel fibers under different CNC content, winding speed and nozzle diameter conditions were fabricated and the correlations of these parameters on fiber diameter were carefully analyzed. The results are summarized in Fig. 6 and Table S2.

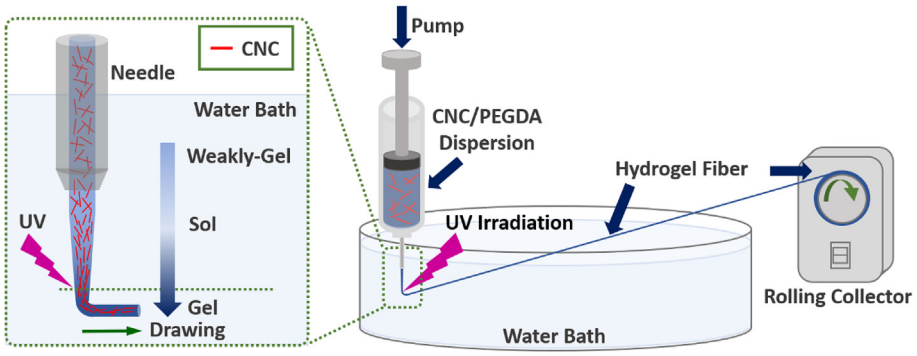

Fig. 3. Schematic illustration of the dynamic-crosslinking-spinning. Enlarged schematic shows the polymerization process under drawing force.

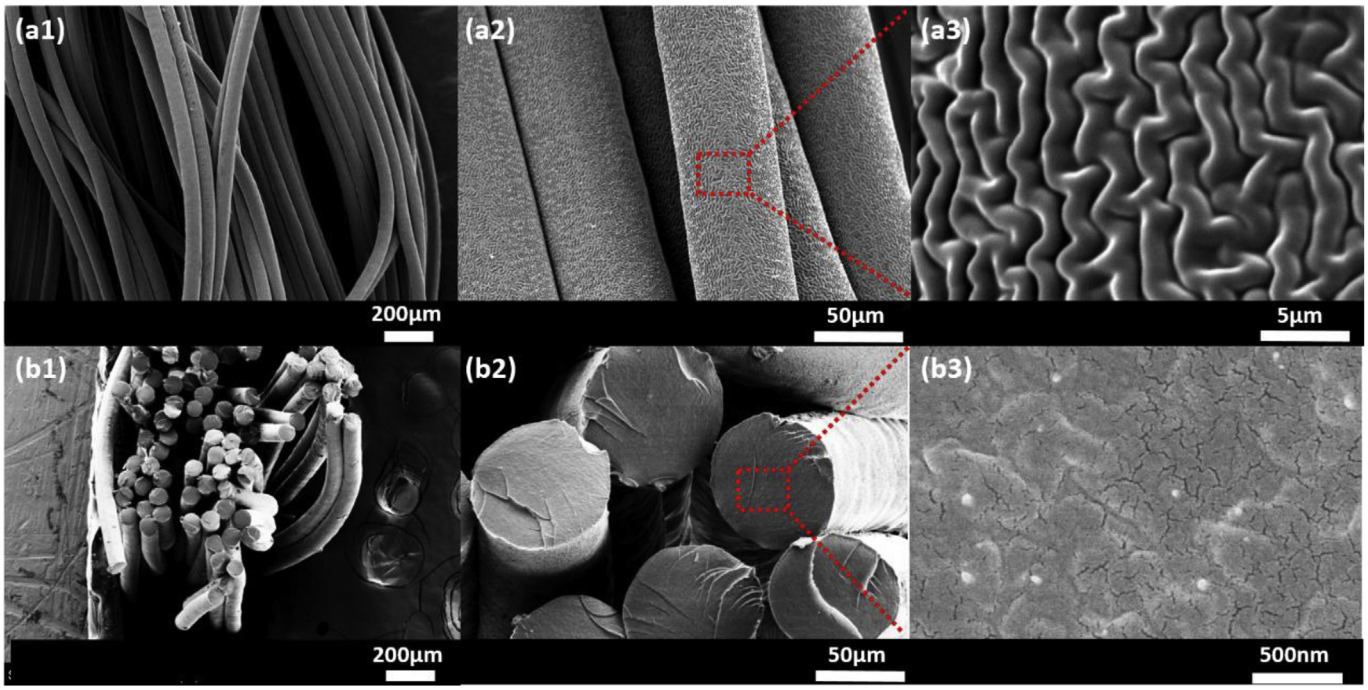

Fig. 4. SEM images of a surface and cross-section morphology of CNC/PEGDA hydrogel fibers in different magnifications.

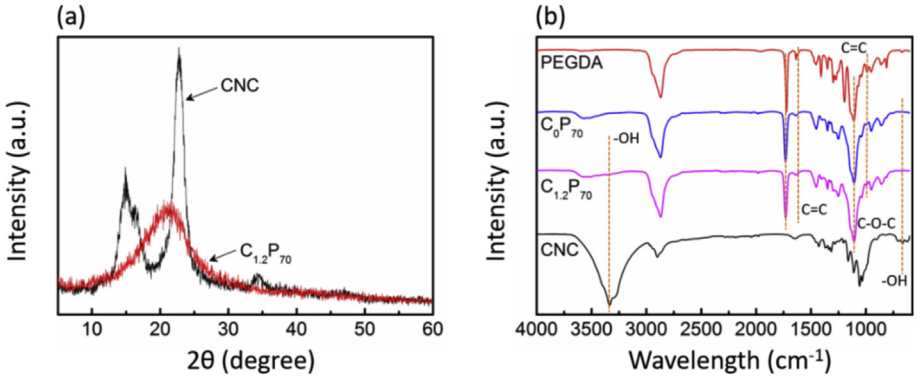

Fig. 5. (a) XRD patterns and (b) FTIR spectra of neat CNC, PEGDA and CNC/PEGDA fibers.

The results indicated that the fiber diameter was scarcely affected by the CNC content under different winding speed condition (Fig. 6a). In addition, under the same shear conditions (extrusion rate = 3.5 ml/h, nozzle diameter = 260 μm), the dispersion viscosity of different CNC content was nearly identical (~10^{-2} pa·s, as in Table S1), indicating the similar fluidity of

different dispersions. Thus, comparing with the ratio of PEGDA in fiber matrix, we concluded that the tiny content of CNC was not able to influence the macroscopic dimension of the fiber.

In one study, the diameter of nanocomposite hydrogel fiber was found to be merely controlled by the nozzle size in 3D printing [11]. However, this was not the case here. For the DCS method, diameter was not affected by the nozzle diameter under the same extrusion and winding conditions as shown in Fig. 6b. The main reason for this observation is that, the viscosity of dispersion extruded from different nozzle were only changed from 0.069 to 0.130 pa·s (Table S1). This tinny difference was not able to influence the fluidity of dispersion, where the amount of dispersion extruded in unit time was about identical. As a result, the diameter of fiber was nearly similar. However, under the same shear condition, we observed that the fiber diameter was influenced by the winding speed according to a power function, which was consist with the relationship we found in neat PEGDA fiber [26]. The above result confirmed that, in order to reduce the influence of CNC addition on the fiber diameter, the viscosity of CNC/PEGDA dispersions with different CNC content could be adjusted to a nearly identical level as the neat PEGDA solution by controlling the extrusion conditions. In this case, the regulating of diameter controlling could become the same as that to produce neat PEGDA fiber.

3.4. Water retention of hydrogel fibers

Hydrogel has been considered as a unique kind of soft material due to its high water retention property. Comparing with bulk hydrogel, hydrogel fiber can exhibit rapid water swelling behavior due to its high surface area/volume ratio (SA:V). In this study, we systematically investigated the effect of CNC content and spinning parameters on the water retention property of CNC/PEGDA hydrogel fiber and the results are shown in Fig. 7.

In Fig. 7a, it was found that the water retention values of all as-prepared fibers were identical, but the retention value decreased by the increasing CNC content in equilibrium swollen fibers. The latter could be explained by the interactions of CNC particles, which formed a physical cross-linked network and thus a denser hydrogel fiber. This compact structure could also be seen by the surface morphology, where the surface roughness could be indicative of the network compactness. It other words, the loose network structure could result in a rougher surface after lyophilization. In Fig S2a, it was seen that the surface became smoother with the increasing in CNC content, indicating the formation of more compact structure formed by the CNC addition and the decreasing tendency of water retention property.

The influence of the winding speed on the water retention property was also investigated and the results are show in Fig. 7b. In this figure, the water retention value was found to be positively correlated with the winding speed. One possible reason is that, the increase in drawing force might cause the collapse of the CNC network, which would be beneficial for improving the water retention property. In addition, the exposure time of the fiber formation under UV irradiation became shorter with the increasing in winding speed, which would reduce the degree of PEGDA polymerization. This would also lead to the increased water retention. The decrease in the crosslink density or the compactness of the fiber by increasing the winding speed was also confirmed by the surface morphology in Fig S2b, of which the surface became rougher with winding speed. Finally, the water retention property of the fiber was found to be independent of nozzle diameter, which was explained earlier. The above results confirmed that the water retention property of CNC/PEGDA hydrogel fiber was closely related to the physical cross-linked structure of CNC particles which could be regulated by the CNC content and winding speed.

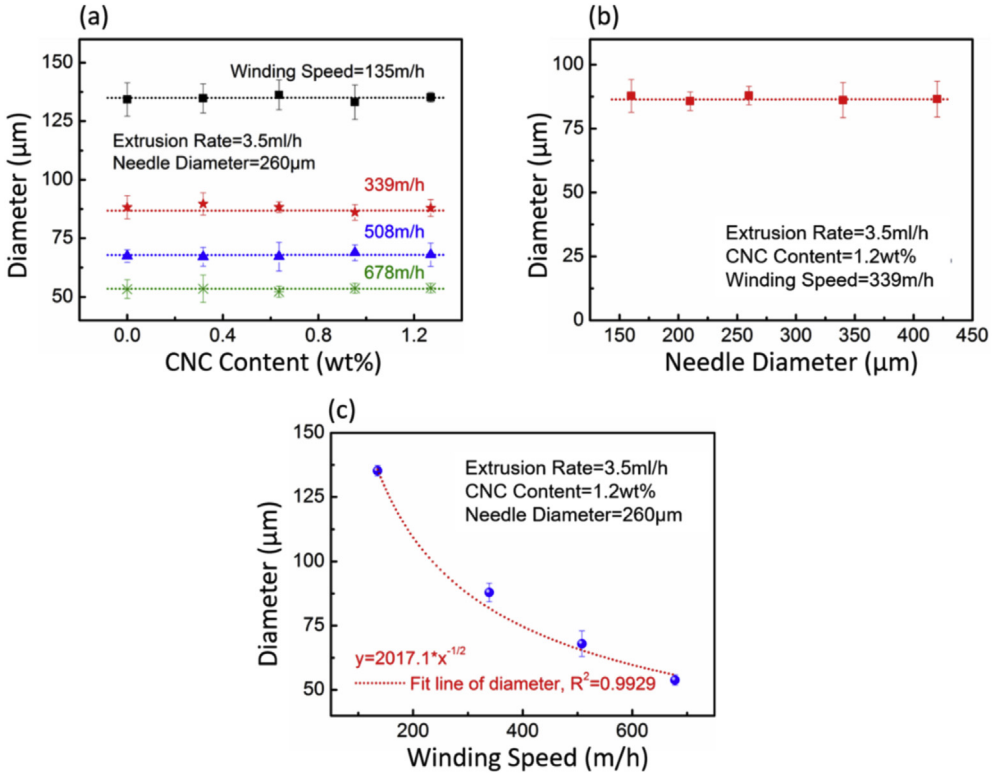

Fig. 6. Dependence of the diameters of the hydrogel fibers on the (a) CNC content, (b) nozzle diameter and (c) winding speed.

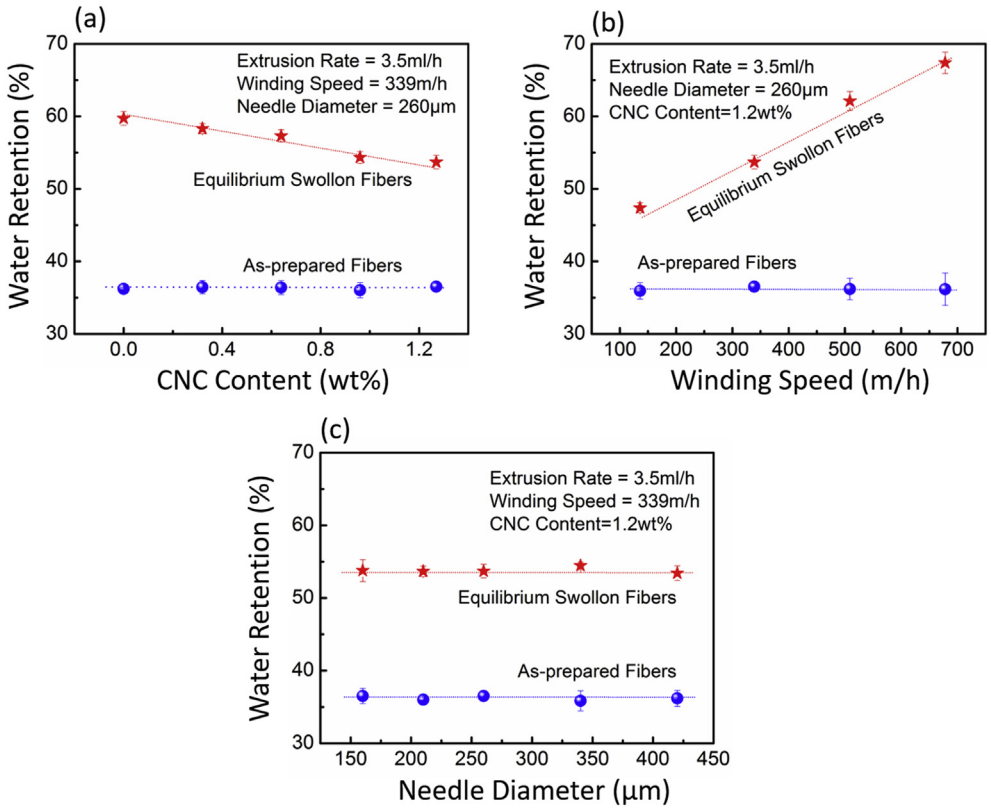

Fig. 7. Dependence of the water retention of the hydrogel fibers on the (a) CNC content and (b) winding speed and (c) nozzle diameter.

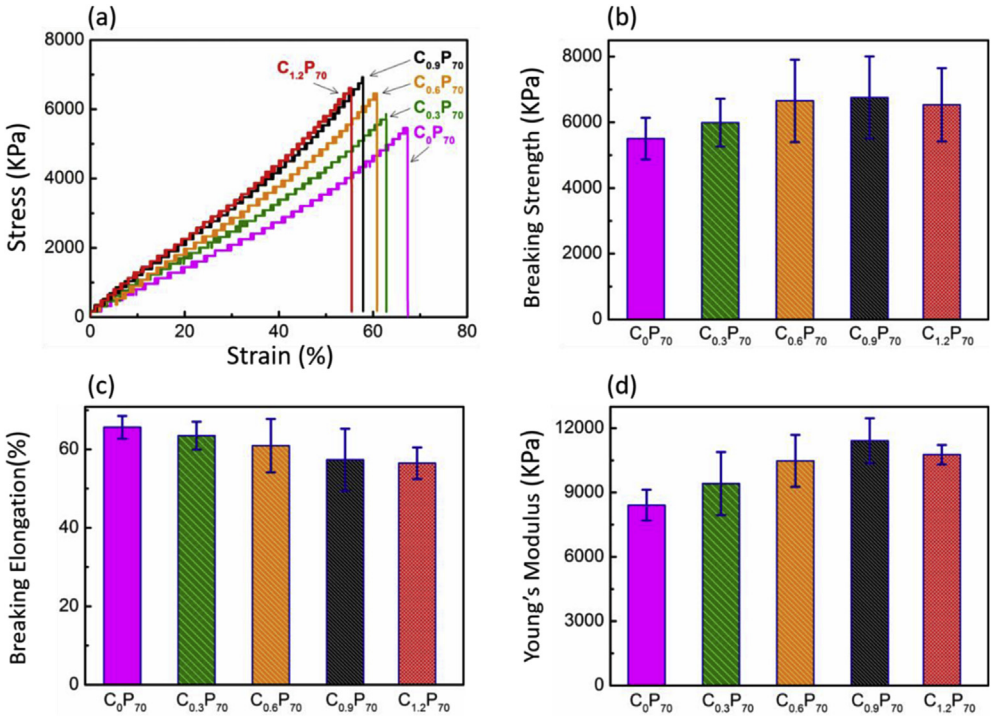

Fig. 8. Mechanical property of CNC/PEGDA hydrogel fibers. Dependence of CNC content on (a) Stress–strain curves of fiber; (b) breaking strength, (c) breaking elongation and (d) young's modulus.

3.5. Mechanical properties of hydrogel fibers

The mechanical properties of CNC/PEGDA fibers with different CNC content are depicted in Fig. 8, which illustrates the breaking elongation (%), breaking strength (KPa) and Young's modulus (KPa), respectively. These results indicated that with the addition of CNC in a relatively small range (0–0.96 wt%), the breaking strength of fiber was improved from 5506 KPa to 6754 KPa, which was consistent the nanoparticle-reinforced property in nanocomposite hydrogel [43]. However, the addition of higher CNC content (1.27 wt%) was found to negatively affect the breaking strength because of the stress-defect point formed by excessive CNC in the fiber matrix that is normally seen nanocomposite fiber [44]. Furthermore, the breaking elongation was negatively correlated with the CNC content because the higher CNC ratio enhanced the crosslinking density that restricted the deformation of hydrogel fiber under tension. The increasing tendency of Young's modulus by the CNC addition could be attributed by the rigidity of the CNC particle, which has been widely utilized as reinforcing filler [45,46].

4. Conclusions

In summary, in order to realize the large-scale production of nanocomposite hydrogel microfibers by non-template dynamic-crosslinking-spinning (DCS) method, systematic rheological investigation of CNC/PEGDA dispersion was carried out. The gelation tendency of the CNC/PEGDA dispersion was generated due to the CNC particle interactions and hydrogen bond formation between CNC and PEGDA. The gelation process is sensitive to the shear force because the CNC/PEGDA dispersion possess the shear thinning behavior. Under the proper extrusion conditions, continuous and uniform CNC/PEGDA hydrogel fibers were successfully fabricated by the DCS method. The diameter and water retention of the hydrogel fibers could be precisely controlled by the CNC content and spinning parameters. Finally, the mechanical property of CNC/PEGDA was found to increase by the addition of CNC. The demonstrated nanocomposite hydrogel fibers could be lead to a new class of useful materials for a broad range of biomedical applications.

Acknowledgements

This research is financially supported by National Key Research and Development Program of China (2016YFA0201702/2016YFA0201700) and Project of Shanghai International Science and Technology Cooperation Fund (14520710200). Prof. Benjamin S. Hsiao also thanks the SusChEM Program of National Science Foundation (DMR-1409507) for the partial financial support.

Appendix A. Supplementary data

Supplementary data related to this article can be found at http://dx.doi.org/10.1016/j.polymer.2017.06.034.

References

[1] T.R. Hoare, D.S. Kohane, Hydrogels in drug delivery: progress and challenges, Polymer 49 (2008) 1993–2007.
[2] M.E. Harmon, M. Tang, C.W. Frank, A microfluidic actuator based on thermoresponsive hydrogels, Polymer 44 (2003) 4547–4556.
[3] A.C. Yu, H. Chen, D. Chan, G. Agmon, L.M. Stapleton, A.M. Sevit, M.W. Tibbitt, J.D. Acosta, T. Zhang, P.W. Franzia, R. Langer, E.A. Appel, Scalable manufacturing of biomimetic moldable hydrogels for industrial applications, P. Natl. Acad. Sci. 113 (2016) 14255–14260.
[4] A. Lendlein, S. Kelch, Shape-memory polymers, Angew. Chem. Int. Ed. 41 (2002) 2034–2057.
[5] J.H. Holtz, S.A. Asher, Polymerized colloidal crystal hydrogel films as intelligent chemical sensing materials, Nature 389 (1997) 829–832.
[6] R. Luo, J. Wu, N.D. Dinh, C.H. Chen, Gradient porous elastic hydrogels with shape-memory property and anisotropic responses for programmable locomotion, Adv. Funct. Mat. 25 (2015) 7272–7279.
[7] M. Akbari, A. Tamayol, V. Laforte, N. Annabi, A.H. Najafabadi, A. Khademhosseini, D. Juncker, Composite living fibers for creating tissue constructs using textile techniques, Adv. Funct. Mat. 24 (2014) 4060–4067.
[8] S. Nemir, H.N. Hayenga, J.L. West, PEGDA hydrogels with patterned elasticity: novel tools for the study of cell response to substrate rigidity, Biotechnol. Bioeng. 105 (2010) 636–644.
[9] Y. Si, X. Wang, C. Yan, L. Yang, J. Yu, B. Ding, Ultralight biomass-derived carbonaceous nanofibrous aerogels with superelasticity and high pressure-sensitivity, Adv. Mat. 28 (2016) 9512–9518.
[10] M. Liu, Y. Ishida, Y. Ebina, T. Sasaki, T. Hikima, M. Takata, T. Aida, An anisotropic hydrogel with electrostatic repulsion between cofacially aligned nanosheets, Nature 517 (2015) 68–72.
[11] A.S. Gladman, E.A. Matsumoto, R.G. Nuzzo, L. Mahadevan, J.A. Lewis, Biomimetic 4D printing, Nat. Mat. 15 (2016) 413–417.
[12] H. Onoe, T. Okitsu, A. Itou, M. Kato-Negishi, R. Gojo, D. Kiriya, K. Sato, S. Miura, S. Iwanaga, K. Kuribayashi-Shigetomi, Y.T. Matsunaga, Y. Shimoyama, S. Takeuchi, Metre-long cell-laden microfibres exhibit tissue morphologies and functions, Nat. Mat. 12 (2013) 584–590.
[13] M. Choi, M. Humar, S. Kim, S.H. Yun, Step-Index optical fiber made of biocompatible hydrogels, Adv. Mat. 27 (2015) 4081–4086.
[14] A.K. Gaharwar, P.J. Schexnailder, A. Dundigalla, J.D. White, C.R. Matos-Perez, J.L. Cloud, S. Seifert, J.J. Wilker, G. Schmidt, Highly extensible bio-nanocomposite fibers, Macromol. Rapid Comm. 32 (2011) 50–57.
[15] J. Su, Y. Zheng, H. Wu, Generation of alginate microfibers with a roller-assisted microfluidic system, Lab. Chip 9 (2009) 996–1001.
[16] D. Lim, E. Lee, H. Kim, S. Park, S. Baek, J. Yoon, Multi stimuli-responsive hydrogel microfibers containing magnetite nanoparticles prepared using microcapillary devices, Soft Matter 11 (2015) 1606–1613.
[17] S. Chen, W. Ma, Y. Cheng, Z. Weng, B. Sun, L. Wang, W. Chen, F. Li, M. Zhu, H.M. Cheng, Scalable non-liquid-crystal spinning of locally aligned graphene fibers for high-performance wearable supercapacitors, Nano Energy 15 (2015) 642–653.
[18] J. Guo, X. Liu, N. Jiang, A.K. Yetisen, H. Yuk, C. Yang, A. Khademhosseini, X. Zhao, S.H. Yun, Highly stretchable, strain sensing hydrogel optical fibers, Adv. Mat. 28 (2016) 10244–10249.
[19] M.A. Daniele, D.A. Boyd, A.A. Adams, F.S. Ligler, Microfluidic strategies for design and assembly of microfibers and nanofibers with tissue engineering and regenerative medicine applications, Adv. Healthc. Mat. 4 (2015) 11–28.
[20] M.A. Daniele, S.H. North, J. Naciri, P.B. Howell, S.H. Foulger, F.S. Ligler, A.A. Adams, Rapid and continuous hydrodynamically controlled fabrication of biohybrid microfibers, Adv. Funct. Mat. 23 (2013) 698–704.
[21] Y. Li, C.T. Poon, M. Li, T.J. Lu, B. Pingguan-Murphy, F. Xu, Chinese-noodle-inspired muscle myofiber fabrication, Adv. Funct. Mat. 25 (2015) 5999–6008.
[22] M.G. Xia, Y.H. Cheng, P. Theato, M.F. Zhu, Thermo-induced double phase transition behavior of physically cross-linked hydrogels based on oligo(-ethylene glycol) methacrylates, Macromol. Chem. Phys. 216 (2015) 2230–2240.
[23] Z.Q. Meng, F. Wei, R.H. Wang, M.G. Xia, Z.G. Chen, H.P. Wang, M.F. Zhu, NIR-laser-switched in vivo smart nanocapsules for synergic photothermal and chemotherapy of tumors, Adv. Mat. 28 (2016) 245–253.
[24] Y. Wu, M. Xia, Q. Fan, M. Zhu, Designable synthesis of nanocomposite hydrogels with excellent mechanical properties based on chemical cross-linked interactions, Chem. Commun. 46 (2010) 7790–7792.
[25] M. Xia, Y. Cheng, Z. Meng, X. Jiang, Z. Chen, P. Theato, M. Zhu, A novel nanocomposite hydrogel with precisely tunable UCST and LCST, Macromol. Rapid Comm. 36 (2015) 477–482.
[26] K. Hou, H. Wang, Y. Lin, S. Chen, S. Yang, Y. Cheng, B.S. Hsiao, M. Zhu, Large scale production of continuous hydrogel fibers with anisotropic swelling behavior by dynamic-crosslinking-spinning, Macromol. Rapid Comm. 37 (2016) 1795–1801.
[27] Y. Zhang, M. Park, H.Y. Kim, S.J. Park, In-situ synthesis of graphene oxide/BiOCl heterostructured nanofibers for visible-light photocatalytic investigation, J. Alloy Compd. 686 (2016) 106–114.
[28] Y. Zhang, M. Park, H.Y. Kim, B. Ding, S.J. Park, In-situ synthesis of nanofibers with various ratios of BiOClx/BiOBry/BiOIz for effective trichloroethylene photocatalytic degradation, Appl. Surf. Sci. 384 (2016) 192–199.
[29] S. Li, S. Hu, W. Jiang, Y. Liu, J. Liu, Z. Wang, Facile synthesis of flower-like Ag_3VO_4/Bi_2WO_6 heterojunction with enhanced visible-light photocatalytic activity, J. Colloid. Interf. Sci. 501 (2017) 156–163.
[30] Z. Meng, F. Wei, R. Wang, M. Xia, Z. Chen, H. Wang, M. Zhu, NIR-laser-switched in vivo smart nanocapsules for synergic photothermal and chemotherapy of tumors, Adv. Mat. 28 (2016) 245–253.
[31] Q. Tian, M. Tang, Y. Sun, R. Zou, Z. Chen, M. Zhu, S. Yang, J. Wang, J. Wang, J. Hu, Hydrophilic flower-like CuS superstructures as an efficient 980 nm laser-driven photothermal agent for ablation of cancer cells, Adv. Mat. 23 (2011) 3542–3547.
[32] Y. Qiu, Z. Ma, P. Hu, Environmentally benign magnetic chitosan/Fe_3O_4 composites as reductant and stabilizer for anchoring Au NPs and their catalytic reduction of 4-nitrophenol, J. Mat. Chem. A 2 (2014) 13471–13478.
[33] V. Guarino, M.A. Alvarez-Perez, A. Borriello, T. Napolitano, L. Ambrosio, Conductive PANi/PEGDA macroporous hydrogels for nerve regeneration, Adv. Healthc. Mat. 2 (2013) 218–227.
[34] B. Lepoittevin, M. Devalckenaere, N. Pantoustier, M. Alexandre, D. Kubies,

C. Calberg, R. Jerome, P. Dubois, Poly(epsilon-caprolactone)/clay nanocomposites prepared by melt intercalation: mechanical, thermal and rheological properties, Polymer 43 (2002) 4017–4023.
[35] S.B. Rossmurphy, Structure-property relationships in food biopolymer gels and solutions, J. Rheol. 39 (1995) 1451–1463.
[36] L.J. Tan, J.P. Pan, A.J. Wan, Shear and extensional rheology of polyacrylonitrile solution: effect of ultrahigh molecular weight polyacrylonitrile, Colloid. Polym. Sci. 290 (2012) 289–295.
[37] Y. Wang, X. Mo, X.S. Sun, D. Wang, Soy protein adhesion enhanced by glutaraldehyde crosslink, J. Appl. Polym. Sci. 104 (2007) 130–136.
[38] H. Tan, W. Gu, D. Liu, J.a. Lu, H. Gao, Sameness and difference of rheological behaviour between sweet potato and mung bean starch pastes, Trans. CSAE 22 (2006) 32–37.
[39] Z. Hu, G. Chen, Aqueous dispersions of layered double hydroxide/polyacrylamide nanocomposites: preparation and rheology, J. Mat. Chem. A 2 (2014) 13593–13601.
[40] C. Spagnol, F.H.A. Rodrigues, A. Neto, A.G.B. Pereira, A.R. Fajardo, E. Radovanovic, A.F. Rubira, E.C. Muniz, Nanocomposites based on poly(acrylamide-co-acrylate) and cellulose nanowhiskers, Eur. Polym. J. 48 (2012) 454–463.
[41] M.G. Xia, W.J. Wu, F.W. Liu, P. Theato, M.F. Zhu, Swelling behavior of thermosensitive nanocomposite hydrogels composed of oligo(ethylene glycol) methacrylates and clay, Eur. Polym. J. 69 (2015) 472–482.
[42] Q. Gao, Z.Y. Qin, C.C. Li, S.F. Zhang, J.Z. Li, Preparation of wood adhesives based on soybean meal modified with PEGDA as a crosslinker and viscosity reducer, BioResources 8 (2013) 5380–5391.
[43] M. Zhu, Y. Liu, B. Sun, W. Zhang, X. Liu, H. Yu, Y. Zhang, D. Kuckling, H.J.P. Adler, A novel highly resilient nanocomposite hydrogel with low hysteresis and ultrahigh elongation, Macromol. Rapid Comm. 27 (2006) 1023–1028.
[44] S.C. Wang, Z. Zhou, H.X. Xiang, W. Chen, E.Q. Yin, T.K. Chang, M.F. Zhu, Reinforcement of lignin-based carbon fibers with functionalized carbon nanotubes, Compos. Sci. Technol. 128 (2016) 116–122.
[45] G. Siqueira, J. Bras, A. Dufresne, Cellulose whiskers versus microfibrils: influence of the nature of the nanoparticle and its surface functionalization on the thermal and mechanical properties of nanocomposites, Biomacromolecules 10 (2009) 425–432.
[46] S.J. Eichhorn, A. Dufresne, M. Aranguren, N.E. Marcovich, J.R. Capadona, S.J. Rowan, C. Weder, W. Thielemans, M. Roman, S. Renneckar, W. Gindl, S. Veigel, J. Keckes, H. Yano, K. Abe, M. Nogi, A.N. Nakagaito, A. Mangalam, J. Simonsen, A.S. Benight, A. Bismarck, L.A. Berglund, T. Peijs, Review: current international research into cellulose nanofibres and nanocomposites, J. Mat. Sci. 45 (2010) 1–33.